Journal of ASTM International, July/August 2005, Vol. 2, No. 7
Paper ID JAI12812
Available online at www.astm.org

E.A. Yamokoski,[1] *B.W. Buczynski,*[1] *N. Stojilovic,*[2] *J.W. Seabolt,*[3] *L.M. Bloe,*[4] *R. Foster,*[4] *N. Zito,*[4] *M.M. Kory,*[5] *R.P. Steiner,*[6] *and R.D. Ramsier*[7]

Influence of Exposure Conditions on Bacterial Adhesion to Zirconium Alloys

ABSTRACT: In this paper we combine surface analytical techniques (X-ray photoelectron spectroscopy, X-ray diffraction, infrared reflection absorption spectroscopy, optical and electron microscopy) with viable counts and statistical ANOVA methods to determine the propensity for biological adhesion on zirconium alloy surfaces. We compare the adhesion of laboratory and clinical strains of *Staphylococcus aureus*, *Staphylococcus epidermidis*, and *Pseudomonas aeruginosa* to Zircaloy-2 and Zircadyne-705 materials. Thermal oxidation of the alloys prior to exposure to biological species is also investigated. We present data for 72-h incubation of bacteria and alloys in both shaken and stationary environments. The results of our statistical analysis and experimental observations are relevant to the use of zirconium-based materials for biomedical applications.

KEYWORDS: zirconium alloys, bacterial adhesion, ANOVA, XPS, FTIR, SEM, optical microscopy

Introduction

The use of zirconium and other refractory metals systems for bio-implants is an active area of research. It has been demonstrated recently that oxidized zirconium surfaces exhibit excellent wear-resistant properties [1–3], making them suitable for hip and knee replacements, for example. Our own studies of these materials began with investigating the growth kinetics of thermally grown oxides on these surfaces [4,5], where we initially focused on pure zirconium and Zircaloy-2 (Zry-2) systems. We then studied, in a preliminary manner, the adhesion behavior of several bacteria on Zry-2 and compared this to adhesion on stainless steel surfaces [6]. There, we demonstrated that oxidized Zry-2 did not promote bacterial adhesion and that the presence of bacteria did not cause oxidation or dissolution of the substrates. These preliminary results led us to the conclusion that bio-inert Zry-2 surfaces can be prepared by simple surface processing methods such as polishing and annealing.

The present paper extends our previous work and presents data and analysis concerning the propensity of clinically relevant *Staphylococcus aureus*, *Staphylococcus epidermidis*, and *Pseudomonas aeruginosa* bacteria to adhere to Zircaloy-2 and Zircadyne-705 (Zr705) surfaces. Here we study both laboratory and clinical strains of the bacteria, shaken and stationary bacteriological exposure conditions, and different surface oxide thicknesses. This choice of

Manuscript received 16 August 2004; accepted for publication 28 December 2004; published July 2005.
[1]Graduate Student, Dept. of Biology, The University of Akron, Akron, OH, 44325.
[2]Graduate Student, Depts. of Physics and Chemistry, The University of Akron, Akron, OH, 44325.
[3]Graduate Student, Dept. of Physics, The University of Akron, Akron, OH, 44325.
[4]Undergraduate Student, Dept. of Physics, The University of Akron, Akron, OH, 44325.
[5]Associate Professor, Dept. of Biology, The University of Akron, Akron, OH, 44325.
[6]Associate Professor, Dept. of Statistics, The University of Akron, Akron, OH, 44325.
[7]Associate Professor, Depts. of Physics, Chemistry, and Chemical Engineering, The University of Akron, Akron, OH, 44325-4001, e-mail: rex@uakron.edu.

bacteria includes those found in hospitals and includes both Gram-positive and -negative genera. We use Fourier transform infrared (FTIR) spectroscopy, X-ray photoelectron spectroscopy (XPS), X-ray diffraction (XRD), optical and electron microscopy, viable counts and statistical analysis of variance (ANOVA) methods, and discuss trends that are both experimentally and statistically significant.

Experimental Details

Substrate Preparation

Zircaloy-2 (nominally 1.4 % Sn, Hf depleted, balance Zr) and Zircadyne-705 (nominally 2.5 % Nb, balance Zr + Hf) sheet stock materials (approximately 1.0 mm thick) were received from Wah Chang and cut into nominally rectangular coupons. The sizes and shapes of the coupons varied, depending on the type of analysis for which they were prepared. For IR and viable counts data the coupons were approximately 20 mm × 48 mm, whereas those for XPS and SEM were much smaller. Each substrate was polished on one side using successively finer diamond pastes followed by 0.05 μm alumina suspension. After ultrasonic cleaning and degreasing with acetone, the samples were placed in Petri dishes until needed. These samples are referred to as metallic. For the oxidized samples referred to in this work, a pre-heated convection furnace was used. Polished and cleaned samples from the Petri dishes were placed in the oven for the desired times, removed with the furnace at temperature, and allowed to cool in air at a relative humidity of approximately 50 %. Annealing temperatures were in the range 500–600°C.

Specular reflection FTIR data were collected with a Mattson 7020 spectrometer in the range 700–4000 cm^{-1} at 4 cm^{-1} resolution for various angles of incidence. Following the procedures outlined in our previous work, the resulting interference fringes were analyzed to determine the thickness of the thermally grown oxide layers [4,5]. The IR beam was p-polarized, the entire bench dry-air purged, and a liquid-nitrogen-cooled HgCdTe detector was used. Front surface gold mirrors provided background data needed for obtaining absorbance spectra.

XRD Measurements

Standard XRD measurements in the 2theta geometry were performed on metallic and oxidized substrates, to verify that our oxidation procedure predominantly yields the expected monoclinic form of zirconium oxide on the surfaces. All of the oxide films studied here were in the pre-transition region of the growth kinetics.

Bacterial Adhesion Protocol

Laboratory and clinical strains of *Staphylococcus aureus*, *Staphylococcus epidermidis*, and *Pseudomonas aeruginosa* were incubated overnight at 37°C in tryptic soy broth (TSB). Each bacterium was separately tested in eight flasks, which contained 250 ml of TSB, 0.5 ml of bacterium, and two sample coupons. A four-flask set was incubated at 37°C, and a separate four-flask set was incubated at 37°C on a shaker. The entire eight-flask set was incubated for three days. The broth was carefully removed from each flask after incubation. One metal coupon per flask was aseptically removed and rinsed for one minute in separate 250 ml beakers of sterile 0.85 % (wt/ml) NaCl. Each rinsed coupon was then put into a tube of sterile 0.85 % NaCl and

vortexed for one minute, allowed to sit for approximately five minutes, and then vortexed for an additional minute. The second coupon in each flask was aseptically rinsed in a corresponding beaker of saline and placed on a sterile piece of bibulous paper in a sterile glass Petri dish for surface analysis.

Viable Counts

The bacteria in the saline tubes were diluted in sterile 0.85 % NaCl and plated using the spread plate technique. Total dilutions of 2×10^1 to 2×10^7 were used and plated on tryptic soy agar (TSA). The plates were incubated at 37°C overnight. Viable counts were reported in bacteria/ml. Before statistical analysis, these data were corrected for the surface area of the sample coupons, since larger coupons would be expected to yield higher viable counts, with all other factors constant. This correction was performed by first weighing each sample and measuring its thickness. Using mass density values of 6.50 and 6.64 g/cm^3 for Zry-2 and Zr705, respectively, we then calculated the surface area of the samples. This procedure neglects the small area represented by the sides of the coupons and the density of the oxide, but these are minor sources of error. This method does, however, account for any variations in the size and shape of the coupons, since all of them were not cut identically.

Surface Analysis Precautions

It is very important for health and safety reasons that a strict protocol be followed by personnel analyzing samples such as those prepared for this study. We list our protocol here for completeness.

- Do not eat, drink or smoke in the room where work is being performed on bacteria-coated coupons.
- Use forceps, and wear disposable gloves when handling the coupons.
- Leave the coupons in the Petri dishes until the analysis is performed.
- Do not remove the filter paper from the Petri dishes.
- After a coupon has been analyzed, return it to the Petri dish.
- Rinse the surface of the instrument that came into contact with the coupons with Lysol. Allow the Lysol to remain on the surface of the instrument for 5 min, then dry it with a paper towel.
- Keep fingers away from the mouth, nose, eyes, or ears while working with the coupons.
- Thoroughly wash hands with warm/hot water and soap after working with the coupons. The washing should take at least 20 s.
- Clean the forceps after each use by spraying with Lysol and washing with warm/hot water and soap.
- Discard the gloves and used paper towels in an autoclave bag labeled as biohazard for proper removal and disposal by health and safety personnel.

FTIR Characterization

Specular reflection measurements of the adsorbed biofilms are performed with the same IR bench used for the oxide film thickness measurements. For studying the biofilms we used a

fixed-angle sampling attachment with gold optics and a polarizer. This provides higher signal-to-noise than the variable angle attachment. In some cases 100 scans or more were averaged as well. For oxidized surfaces, the large intensity interference peaks obscure those from the adsorbed bacteria. However, we do present data below from metallic samples with and without bacteria.

XPS Analysis

The XPS analysis was performed in fixed analyzer transmission mode under high vacuum conditions with pressures often below 8×10^{-9} Torr. We used a Kratos ES-300 electron spectrometer with a dual anode source. For all measurements, the aluminum source was used for the primary survey and detail scans, however the magnesium anode was selected to verify the identity of some Auger features. The X-ray source was operated at 12 kV and 10 mA with the samples approximately 1 cm away from the source. Samples were mounted onto the end of a probe and inserted into a load-lock sample transfer flange for analysis. Argon ion suttering was performed to remove surface contamination and also to further remove material. The sputtering gun was focused and rastered and operated at 2.5 kV. Ultra-high purity argon gas at a total pressure of 2×10^{-5} Torr was used, which corresponds to a sputtering rate of a gold standard of approximately 0.63 nm/min. Depth-profiling values are with respect to this gold standard, and we have not determined differential sputtering rates in this study.

Optical and Electron Microscopy Observations

Microscopic imaging of some of the surfaces was performed with standard optical and SEM techniques. Low-power optical microscopes were used to observe colony formation, and SEM operating at 25 kV was used for identifying bacteria individually. Gold was sputter-coated onto the surfaces to reduce charging effects in SEM measurements.

Results and Discussion

XRD Verification of Substrate Structure

Figure 1 presents representative XRD patterns obtained from the substrates used in this study. Not surprisingly, the strong diffraction peaks from the metallic alpha-Zr phase material (Zr705 in this case) are replaced by monoclinic-ZrO_2 features after thermal oxidation in air [7–9]. The main peaks are from the (-111) and (200) planes and are labeled in the figure with m-ZrO_2 signifying the monoclinic-form of the oxide. There is no evidence for tetragonal-phase zirconia, consistent with what we expect from the literature. All of the oxides layers studied here are in the range before the transition region in the growth kinetics. The thickest oxide layers as determined by IR in this study are 3.1 μm, and all the diffraction patterns that we recorded were similar to those shown in Fig. 1. The two diffraction patterns shown in Fig. 1 have been vertically shifted for clarity of presentation.

Specular IR Reflectance from Surfaces

Specular reflectance IR spectra from metallic Zry-2 surfaces are presented in Fig. 2, where we focus on the region containing the amide modes [10–13]. The lower spectrum is from a

coupon exposed for three days to TSB only and serves as a control for our detection of bacterial IR signatures. Both of the spectra in Fig. 2 are from samples exposed to *S. epidermidis* in TSB for the same time period, and clearly show amide II (1555 cm^{-1}) and amide I (1670 cm^{-1}) bands. Note that the intensities of the features from the sample that was shaken during exposure are slightly higher than those from the stationary sample. This observation indicates that more bacteria adhered during shaking and is supported by the ANOVA analysis discussed below. The spectra in Fig. 2 have been vertically shifted for clarity, but no baseline corrections have been made. As mentioned in Section 2, single-pass IR reflection spectroscopy was not able to identify bacteria on oxidized surfaces, since the interference features dominate the spectra [4–6].

XPS Analysis

XPS survey scans are shown in Fig. 3, where the spectra are once again vertically shifted for clarity. Figure 3*a* is from metallic Zr705, before sputter cleaning. The main features present are from zirconium, oxygen, and carbon, as expected. Spectrum 3B is from a similar sample exposed to TSB for three days per the protocol described in Section 2. Note the attenuation of the Zr features and the increase in intensity of the O and C signatures. Traces of phosphorus, nitrogen, and sodium are also evident. This serves as a control for our detection of bacteria by XPS. Finally, spectrum 3C results from a metallic Zr705 surface exposed to *Pseudomonas aeruginosa* in TSB for three days. Note the significant decrease in the Zr features and a further increase in the carbon and sodium signals. Chlorine is also now apparent, and the O(1s) feature is significantly broadened on the high-energy side.

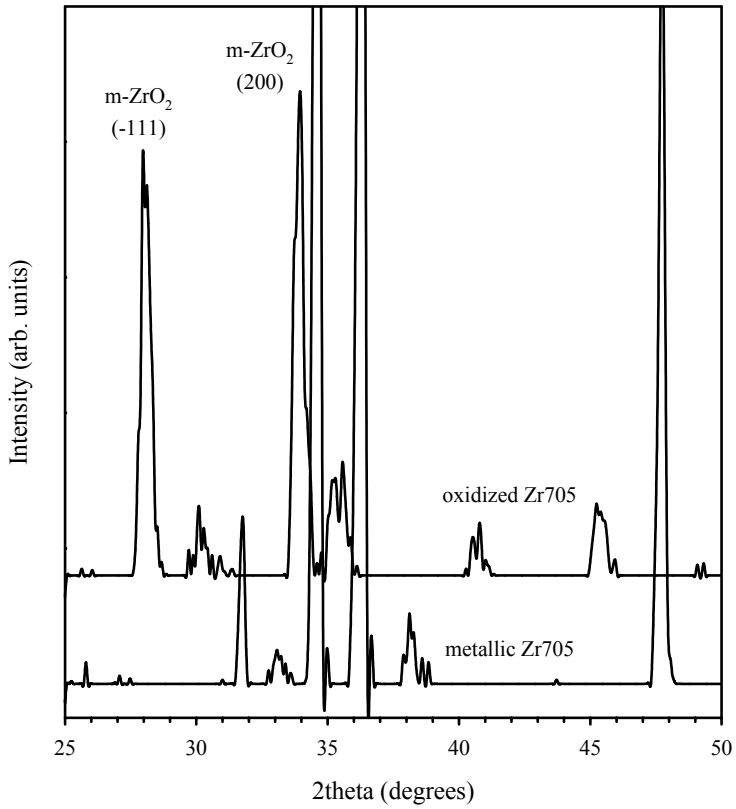

FIG. 1—*X-ray diffraction patterns from metallic and oxidized Zr705, with the latter demonstrating the monoclinic zirconia phase.*

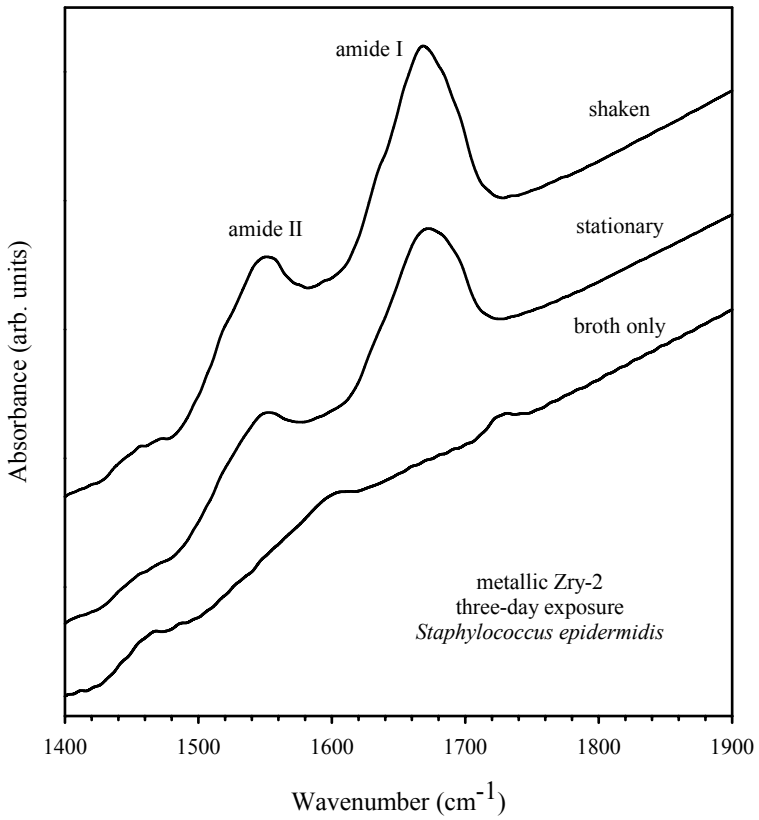

FIG. 2—*Specular reflection IR spectra from metallic Zry-2 surfaces, showing 1555 cm^{-1} amide II and 1670 cm^{-1} amide I bands. Note that these bands are not present from the broth, and that shaken exposure yields slightly more intense bacterial signatures in this case than stationary exposure.*

The decrease in the Zr features due to scattering by adsorbates is a consistent trend that we have observed, similar to the study by Rubio, et al. [13]. The Na and Cl features in our spectra are due to the saline solution used in the sample preparation, and it is clear that much more NaCl resides on surfaces that contain bacteria than on those without biological species. We also observe this in the microscopy studies discussed below. The fact that the C(1s) peak in Fig. 3 also increases with bacterial exposure is consistent with the adhesion of bacteria. Of specific interest here is the O(1s) line, shown in a set of detailed scans in Fig. 4. Here, we see that sputtering removes the high-energy shoulder, which is attributed to oxygen-carbon bonds in the microbial cell surfaces [14]. Sputtering for 30 and 150 min corresponds to the removal of approximately 19 and 95 nm of material, respectively. The latter value is the same order of magnitude as the cell wall thickness of this bacterium, so the observed changes in the spectra are understandable.

Optical Imaging

Optical microscopy proved to be very interesting in this work as well. Many of the samples examined had no observable bacterial growth anywhere on the surface, especially the oxidized coupons. It seemed that metallic surfaces had a higher density of bacteria. The viable counts data did indicate more adhesion on metallic surfaces than on oxidized surfaces, especially for

Pseudomonas aeruginosa, but these observations were not statistically significant. Nevertheless, bacterial adhesion was identified in some cases optically. An example of such a case is given in Fig. 5, which shows *Staphylococcus epidermidis* on an oxidized Zr705 surface in a fractal-like growth pattern.

SEM Studies

Sparse bacterial adhesion on many of the surfaces was verified by SEM imaging. Figure 6 shows one such image, which we present to focus attention on surface defects. This is an oxidized Zr705 surface that was exposed to *Pseudomonas aeruginosa* for three days in a shaken environment. Note that the bacteria have a rod-like appearance, consistent with what has been reported by others [15]. This image and others like it indicate that the bacteria are not preferentially adsorbed in regions of surface defects. This is an interesting result from the standpoint of the effects of surface preparation on bacteriological adhesion to zirconium alloys. We have analyzed other SEM images of oxidized Zr705 surfaces exposed to *Pseudomonas aeruginosa* for up to one month under stationary conditions. Most of these surfaces are void of bacteria, indicating that even long exposures under stationary conditions is not as effective for bacterial growth as are short times with shaking. This observation is consistent with our ANOVA data as well.

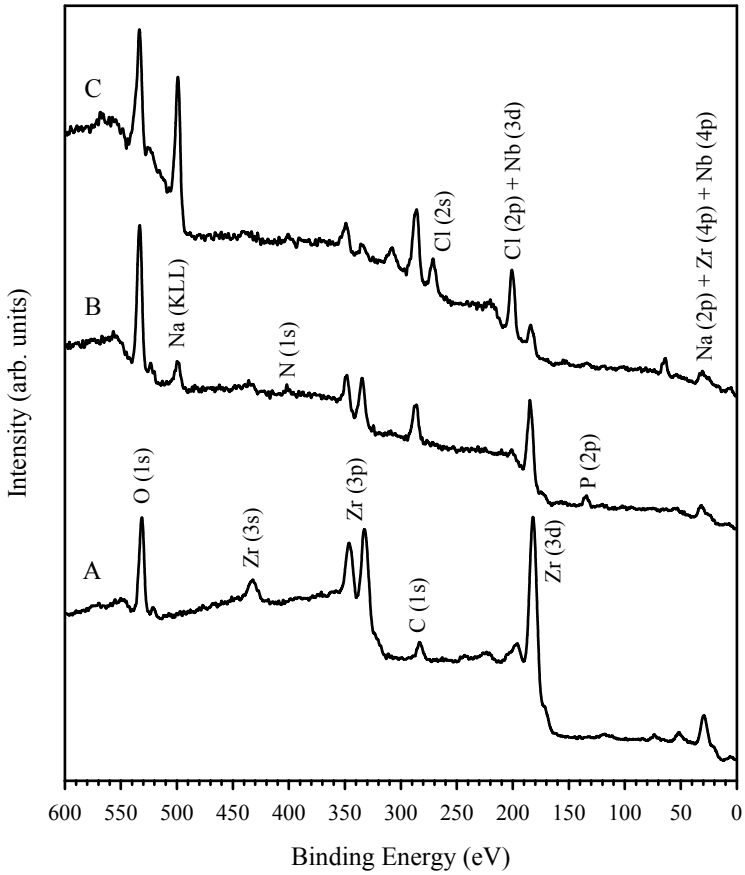

FIG. 3—*X-ray photoelectron survey spectra of metallic Zr705, (A) as polished and cleaned, (B) exposed to broth only, and (C) exposed to Pseudomonas aeruginosa under shaken conditions.*

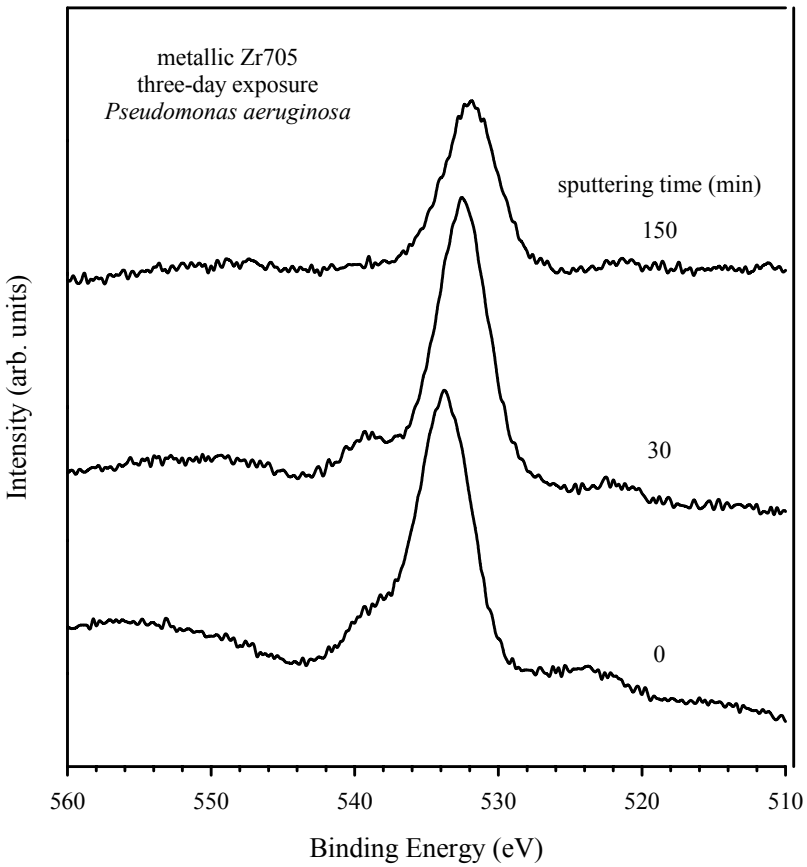

FIG. 4—*The O(1s) region of the upper spectrum of Fig. 3 and the effects of argon ion sputtering.*

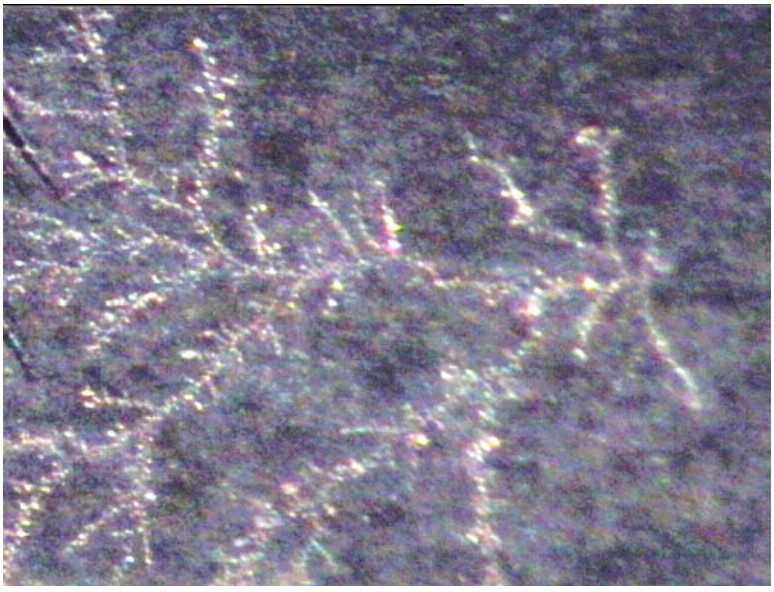

0.1 mm

FIG. 5—*Optical image of a fractal-like colony of Staphylococcus epidermidis on an oxidized Zr705 substrate. The arrow beneath the figure represents 0.1 mm.*

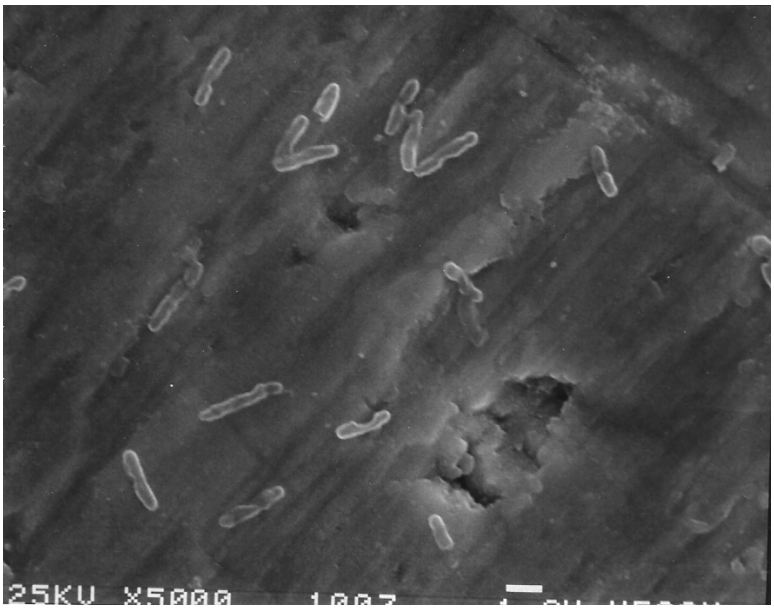

FIG. 6—*SEM image of Pseudomonas aeruginosa bacteria on an oxidized Zr705 substrate after exposure for three days while shaking. There seems to be no enhanced adhesion near defects. The inset scale bar is 1 μm.*

Statistical ANOVA Studies

Adhesion on Zry-2—The data were analyzed using a four-factor ANOVA. The factors were Bacterium (Staphylococcus aureus, Staphylococcus epidermidis, and Pseudomonas aeruginosa), Strain (clinical, laboratory), Condition (shaken, stationary), and Oxidation thickness (0, 1.7, 2.2 μm). The response variable was bacterial growth measured as ln(viable counts/ml/cm^2). The natural logarithm transformation of growth was used to satisfy the ANOVA requirements of normally distributed data with equal variability across factor levels.

First, a model including main effects for each factor and two- and three-factor interactions was tested. It was assumed that there was no interaction simultaneously involving all four factors, thus the mean square for this interaction effect was used as the error for testing the effects in the model. In this analysis, none of the three-factor interactions, nor any effects involving oxidation thickness, contributed meaningfully to the model (P-values ranged from 0.32 to 0.86). Therefore, a second ANOVA model was analyzed that included only main effects for Bacterium, Strain, Condition and their two-factor interactions.

This model (mean square error = 1.63, error df = 25) formed the primary basis of our statistical analysis. In this model, there was a statistically significant Strain x Bacterium interaction (P = 0.005), which indicated that the clinical strain of *P. aeruginosa* exhibited more growth than the lab strain of *P. aeruginosa*. Clinical and laboratory strains of *S. aureus* did not differ significantly from one another, nor did clinical and laboratory strains of *S. epidermidis* differ significantly. Thus, a strain effect existed for *P. aeruginosa* only. The results of this analysis are presented in Fig. 7, in which the data for shaken and stationary conditions are combined.

Another result is that for all bacteria and all strains, there was greater growth under shaken conditions than for stationary conditions (main effect for Condition, P<0.0001). This is demonstrated in Fig. 8. In addition, a Strain x Condition interaction also was found (P = 0.04).

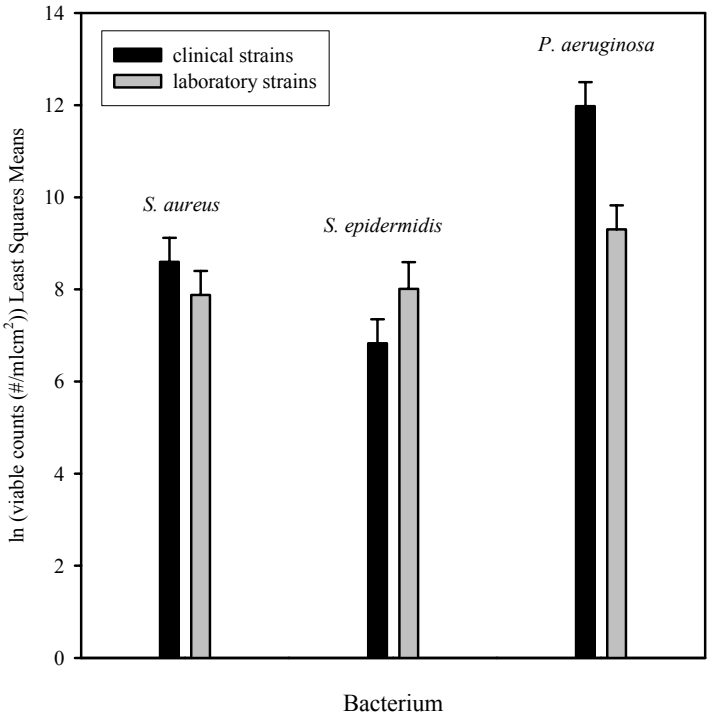

FIG. 7—*Data from ANOVA analysis that indicate a statistically significant difference in the adhesion ability of the three bacteria (*Pseudomonas aeruginosa > Staphylococcus aureus > Staphylococcus epidermidis*) and that in the first case the use of clinical strains enhanced the bacteriological growth.*

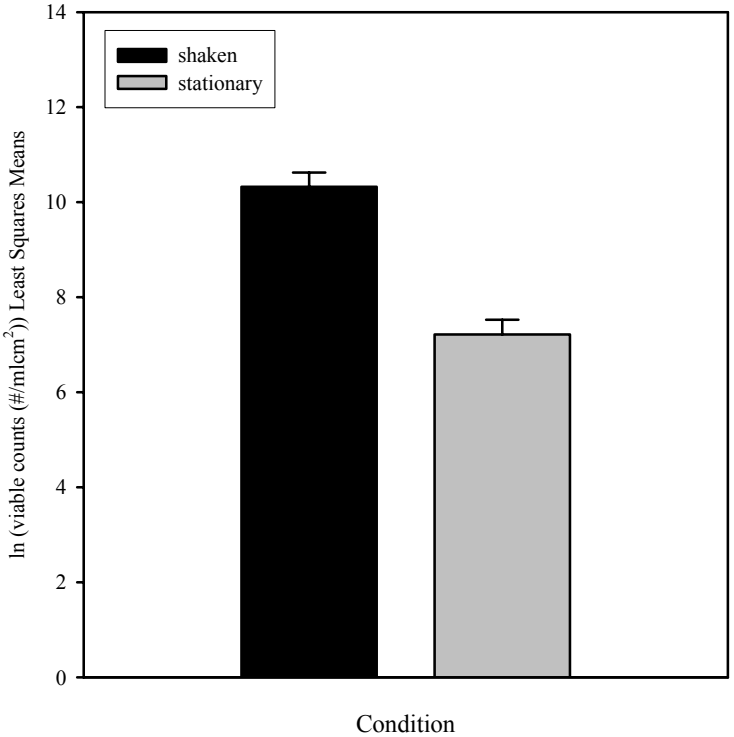

FIG. 8—*Data from ANOVA analysis that indicate a statistically significant difference between stationary and shaken conditions with respect to the adhesion ability of the three bacteria.*

Under shaken conditions, clinical and laboratory strains exhibited very similar growth, but laboratory strains exhibited a greater reduction in growth than clinical strains under stationary conditions. The three species of bacteria also differed in overall mean growth (main effect of Bacterium, $P< 0.0001$). Specifically, *P. aeruginosa* exhibited more growth than *S. aureus*, which in turn exhibited more growth than *S. epidermidis* (Tukey's HSD multiple comparisons procedure at the 0.05 level of significance). Although not statistically significant ($P= 0.28$), the observed Bacterium x Condition interaction suggests that *S. aureus* may exhibit a greater reduction in growth under stationary conditions than either *P. aeruginosa* or *S. epidermidis*. The latter two organisms show similar declines (compared to each other) under stationary conditions. These effects are also apparent in Fig. 7.

Adhesion on Zry-2 vs. Zr705—The two materials were analyzed using a four-factor ANOVA. The factors were Bacterium (Staphylococcus aureus, Staphylococcus epidermidis, and Pseudomonas aeruginosa), Strain (clinical, laboratory), Condition (shaken, stationary), and Material (Zry-2 vs. Zr705). All samples analyzed had 2.2 μm oxide thickness. Again, the response variable was bacterial growth measured as ln(viable counts/ml/cm^2). First, a model including main effects for each factor and all two-factor interactions was tested. In this analysis, the Material x Strain ($P = 0.73$) and Material x Bacterium ($P = 0.64$) interactions did not contribute meaningfully to the model. So, as before, a second ANOVA model was analyzed with these effects excluded.

The analysis of this model (mean square error = 0.75, error df = 10) led to results for effects *not* involving Material that were similar to those observed in the analysis of Zircaloy-2 alone. Therefore, only the results for effects involving Material are discussed here. Although not statistically significant, we observed less growth on Zr705 than on Zircaloy-2 (main effect of Material, $P = 0.06$). Also, there was a nearly significant ($P = 0.08$) Material x Condition interaction, which suggested that both materials exhibit similar growth under stationary conditions. However, while growth is larger on both materials under shaken conditions, the increase in growth is less for Zr705. See Table 1 for a summary of the samples used in this study.

TABLE 1—*Batches of samples exposed to bacteria for three days studied in this work. Here, L stands for laboratory strains and C for clinical strains in parentheses. The abbreviations for the bacteria are SA, SE, and PA, corresponding to* Staphylococcus aureus*,* Staphylococcus epidermidis*, and* Pseudomonas aeruginosa*, respectively.*

Substrate	Oxide Thickness (μm)	Bacterium (strain)	Condition	Viable Counts (#/mlcm^2) × 10^{-3}
Zr705	0.0	PA (L)	shaken	2.45
Zr705	0.0	PA (L)	shaken	2.63
Zr705	1.8	PA (L)	shaken	7.92
Zr705	1.6	PA (L)	shaken	5.16
Zr705	1.7	PA (L)	shaken	6.20
Zr705	2.1	PA (L)	shaken	3.18
Zr705	2.1	PA (L)	shaken	5.58
Zr705	3.1	PA (L)	shaken	7.30
Zr705	2.0	PA (L)	shaken	69.6
Zr705	2.1	PA (L)	shaken	3.62
Zry-2	0.0	SA(L)	stationary	1.12
Zry-2	1.7	SA(L)	stationary	0.24
Zry-2	2.2	SA(L)	stationary	0.07
Zr705	2.2	SA(L)	stationary	…

Substrate	Oxide Thickness (μm)	Bacterium (strain)	Condition	Viable Counts (#/mlcm^2) × 10^{-3}
Zry-2	0.0	SE(L)	stationary	0.18
Zry-2	1.7	SE(L)	stationary	…
Zry-2	2.2	SE(L)	stationary	0.45
Zr705	2.2	SE(L)	stationary	0.16
Zry-2	0.0	PA(L)	stationary	20.1
Zry-2	1.7	PA(L)	stationary	0.60
Zry-2	2.2	PA(L)	stationary	0.75
Zr705	2.2	PA(L)	stationary	0.55
Zry-2	0.0	SA(L)	shaken	20.6
Zry-2	1.7	SA(L)	shaken	11.5
Zry-2	2.2	SA(L)	shaken	74.6
Zr705	2.2	SA(L)	shaken	9.94
Zry-2	0.0	SE(L)	shaken	24.5
Zry-2	1.7	SE(L)	shaken	56.8
Zry-2	2.2	SE(L)	shaken	11.2
Zr705	2.2	SE(L)	shaken	16.0
Zry-2	0.0	PA(L)	shaken	145
Zry-2	1.7	PA(L)	shaken	5.55
Zry-2	2.2	PA(L)	shaken	241
Zr705	2.2	PA(L)	shaken	10.5
Zry-2	0.0	SA(C)	stationary	1.40
Zry-2	1.7	SA(C)	stationary	0.24
Zry-2	2.2	SA(C)	stationary	2.67
Zr705	2.2	SA(C)	stationary	4.13
Zry-2	0.0	SE(C)	stationary	0.39
Zry-2	1.7	SE(C)	stationary	2.64
Zry-2	2.2	SE(C)	stationary	0.49
Zr705	2.2	SE(C)	stationary	…
Zry-2	0.0	PA(C)	stationary	75.3
Zry-2	1.7	PA(C)	stationary	27.8
Zry-2	2.2	PA(C)	stationary	30.2
Zr705	2.2	PA(C)	stationary	53.7
Zry-2	0.0	SA(C)	shaken	104
Zry-2	1.7	SA(C)	shaken	9.86
Zry-2	2.2	SA(C)	shaken	27.5
Zr705	2.2	SA(C)	shaken	38.2
Zry-2	0.0	SE(C)	shaken	0.86
Zry-2	1.7	SE(C)	shaken	0.35
Zry-2	2.2	SE(C)	shaken	4.16
Zr705	2.2	SE(C)	shaken	0.18
Zry-2	0.0	PA(C)	shaken	467
Zry-2	1.7	PA(C)	shaken	792
Zry-2	2.2	PA(C)	shaken	701
Zr705	2.2	PA(C)	shaken	145

Summary Comments

In this work we tested the ability of clinically relevant *Staphylococcus aureus*, *Staphylococcus epidermidis*, and *Pseudomonas aeruginosa* bacteria to adhere to Zircaloy-2 and Zircadyne-705 surfaces. We demonstrated through the use of viable counts methods that bacterial adhesion to these metal surfaces depends mainly on the exposure conditions (shaken or stationary) and the bacterium of interest. While only significant for *Pseudomonas aeruginosa*, the bacterial strain (clinical origin) also enhances adhesion. To a lesser extent, the specific alloy may make a difference as well. Here we have found no conclusive evidence that surface oxidation enhances or mitigates bacteriological growth. However, it is clear that in the present study, while the samples were being shaken, bacteriological exposures resulted in more growth than for stationary samples. This differs from what we have previously reported on other substrates, however we are using clinical strains in this study. We are currently planning a set of experiments similar to those described here, but with a different collection of clinical strains, to determine if bacterial aggressiveness is related to their original source.

Our XRD data indicate that the surfaces we are studying are either metallic or fully oxidized, and our IR spectra exhibit the amide signatures of adsorbed bacteria in some cases involving metallic substrates. XPS results demonstrate the presence of adsorbed bacteria, especially through the shape and position of the O(1s) feature. Optical microscopy shows that in some cases, macroscopic colonies of bacteria form on these surfaces via fractal-like growth mechanisms. SEM has shown that bacteria do not preferentially adsorb at surface defects, which is another interesting result that needs further investigation. Overall, the data that we have collected thus far indicate that zirconium alloys are relatively inert toward bacterial adhesion and constitute a biocompatible class of materials for use by the biomedical community.

Acknowledgments

We acknowledge support for this effort through NIH-NIBIB grant number EB003397-01, and we are grateful to Wah Chang for providing the Zry-2 and Zr705 materials free-of-charge. We are also appreciative of the assistance provided by Jeannette Killius of the Northeastern Ohio Universities College of Medicine with the SEM phases of this work, and for access to the optical microscope by Professor George Chase.

References

[1] Good, V., Ries, M., Barrack, R. L., Widding, K., Hunter, G., and Heuer, D., "Reduced Wear with Oxidized Zirconium Femoral Heads," *Journal of Bone and Joint Surgery*, American Vol. 85A, 105, Suppl. 4, 2003.

[2] Ries, M. D., Salehi, A., Widding, K., and Hunter, G., "Polyethylene Wear Performance of Oxidized Zirconium and Cobalt-Chromium Knee Components under Abrasive Conditions," *Journal of Bone and Joint Surgery*, American Vol. 84A, 129, Suppl. 2, 2002.

[3] Heuer, D., Harrision, A., Gupta, H., and Hunter, G., "Chemically Textured and Oxidized Zirconium Surfaces for Implant Fixation," *Bioceramics 15 Key Engineering Materials*, 240–2, 789, 2003.

[4] Morgan, J. M., McNatt, J. S., Shepard, M. J., Farkas, N., and Ramsier, R. D., "Optical and Structural Studies of Films Grown Thermally on Zirconium Surfaces," J*ournal of Applied Physics 91*, 9375, 2002.

[5] McNatt, J. S., Shepard, M. J., Farkas, N., Morgan, J. M., and Ramsier, R. D., "Non-Destructive Characterization of Films Grown on Zircaloy-2 by Annealing in Air," *Journal of Physics D*, Applied Physics 35, 1855, 2002.
[6] Buczynski, B. W., Kory, M. M., Steiner, R. P., Kittinger, T. A., and Ramsier, R. D., "Bacterial Adhesion to Zirconium Surfaces," *Colloids and Surfaces B: Biointerfaces 30*, 167 2003.
[7] Baek, J. H. and Jeong, Y. H., "Depletion of Fe and Cr within Precipitates During Zircaloy-4 Oxidation," *Journal of Nuclear Materials 304*, 107, 2002.
[8] Kim, H. G, Kim, T. H. ,and Jeong, Y. H., "Oxidation Characteristics of Basal (0002) Plane and Prism (11-20) Plane in HCP Zr," *Journal of Nuclear Materials 306*, 44, 2002.
[9] Huy, L. D., Laffez, P., Daniel, Ph., Jouanneaux, A., Khoi, N. T., and Simeone, D., "Structure and Phase Component of ZrO_2 Thin Films Studied by Raman Spectroscopy and X-ray Diffraction," *Materials Science and Engineering B 104*, 163, 2003.
[10] Ede, S. M., Hafner, L. M., and Fredericks, P. M., "Structural Changes in the Cells of Some Bacteria During Population Growth: A Fourier Transform Infrared-Attenuated Total Reflectance Study," *Applied Spectroscopy 58*, 317, 2004.
[11] Reiter, G., Siam, M., Falkenhagen, D., Gollneritsch, W., Baurecht, D., and Fringeli, U. P., "Interaction of a Bacterial Endotoxin with Different Surfaces Investigated by in Situ Fourier Transform Infrared Attenuated Total Reflection Spectroscopy," *Langmuir 18*, 5761, 2002.
[12] Filip, Z. and Hermann, S., "An Attempt to Differentiate *Pseudomonas* spp. and Other Soil Bacteria by FT-IR Spectroscopy," *Eur. J. Soil Biol. 37*, 137, 2001.
[13] Rubio, C., Costa, D., Bellon-Fontaine, M. N., Relkin, P., Pradier, C. M., and Marcus, P., "Characterization of Bovine Serum Albumin Adsorption on Chromium and AISI 304 Stainless Steel, Consequences for the *Pseudomonas fragi* K1 Adhesion," *Colloids and Surfaces B: Biointerfaces 24*, 193, 2002.
[14] Van der Mei, H. C., de Vries, J., and Busscher, H. J., "X-Ray Photoelectron Spectroscopy for the Study of Microbial Cell Surfaces," *Surface Science Reports 39*, 1, 2000.
[15] Reid, G., Busscher, H. J., Sharma, S., Mittelman, M. W., and McIntyre, S., "Surface Properties of Catheters, Stents and Bacteria Associated with Urinary Tract Infections," *Surface Science Reports 21*, 251, 1995.